biomass

MDPI

Article

Modeling the Retting of Linseed Straw with Controlled Humidification and Consideration of the Microbiota Composition

Olga Gorach [1,*], Sergiy Lavrenko [2] and Nataliia Lavrenko [3]

[1] Department of Food Technology, Kherson State Agrarian and Economic University, 73006 Kherson, Ukraine
[2] Department of Agriculture, Kherson State Agrarian and Economic University, 73006 Kherson, Ukraine; lavrenko_s@ksaeu.kherson.ua
[3] Department of Land Management, Geodesy and Cadastre, Kherson State Agrarian and Economic University, 73006 Kherson, Ukraine; lavrenko_n@ksaeu.kherson.ua
* Correspondence: horach_o@ksaeu.kherson.ua

Abstract

The aim of this study was to investigate the patterns governing the conversion of oilseed flax straw into retted straw under the climatic conditions of southern Ukraine through examining moisture absorption, moisture desorption, and the associated microbiological processes. It was established that stem moisture content approaching 100% is reached within 10 min of moistening, after which the process shifts from adsorption of free water to absorption of bound water. Analysis of the moisture desorption curves demonstrated that a single moistening event is insufficient to sustain the moisture level required for active microbial proliferation, as moisture content decreases by approximately 45% within the first hour and gradually reverts to baseline values thereafter. The mathematical modeling results indicate that without supplementary moistening, the biological conversion of straw into retted straw is virtually negligible. It was found that twice-daily moistening promotes the dominance of pectinolytic microorganisms, ensuring efficient breakdown of pectic substances and the formation of high-quality retted straw. However, after 5–6 days of retting, a sharp increase in the numbers of cellulolytic and pathogenic microflora is observed, which may lead to degradation of the cellulose complex and deterioration of fiber properties. The obtained findings can be used to optimize bast biomass processing technologies, develop predictive systems for the retting process, and improve the quality of the resulting fiber.

Keywords: oilseed flax; bast biomass; retted straw; mathematical modeling; process forecasting; moisture absorption; artificial moistening; microbiota; pectinolytic microorganisms; fiber quality

Check for updates

Academic Editor: Florent Allais

Received: 28 August 2026
Revised: 9 October 2026
Accepted: 12 October 2026
Published: 14 October 2026

Copyright: © 2026 by the authors. Licensee MDPI, Basel, Switzerland. This article is an open access article distributed under the terms and conditions of the Creative Commons Attribution (CC BY) license.

1. Introduction

Recent research on flax retting has shifted from empirical field practice toward characterization of the microbial community, degradation of pectin and hemicellulose, and quantitative monitoring of retting progress. Metagenomic, metaproteomic, spectroscopic, and multimodal studies have shown that retting is a dynamic microbiological process in which changes in the plant cell-wall matrix and microbial community are closely related to fiber quality [1–6]. Recent work has also demonstrated that microbial communities can be steered by environmental conditions or microbial additions and that the duration of retting affects the mechanical properties of the resulting fibers [7–9].

A consistent finding across these studies is that moisture availability is a major determinant of dew-retting kinetics. Moisture regulates microbial establishment and activity,

while prolonged wetting can shift the process from selective degradation of intercellular pectic substances toward less desirable degradation of structural polysaccharides. Accordingly, recent studies have increasingly combined microbiological measurements with process-duration or material-quality indicators rather than treating retting as a purely visual or time-based operation [7–12]. Recent work using high-throughput sequencing and spectroscopic methods likewise shows that the succession of functional microbial taxa is associated with changes in the sequence of pectin, hemicellulose, and other cell-wall component degradation [13].

Despite this progress, most mechanistic and process-monitoring studies concern fiber flax or controlled retting systems, whereas the conversion of oilseed flax straw into retted straw remains insufficiently characterized. Previous work on oilseed flax has primarily addressed seed utilization or direct fiber recovery from straw; comparatively little attention has been given to biological preparation of oilseed flax straw before fiber extraction [14–16]. This distinction is important because oilseed flax straw is produced in large quantities as a by-product of seed production, yet its field retting behavior may differ from that of fiber flax under dry continental conditions.

Dew retting is particularly sensitive to temperature and moisture conditions. The available literature identifies pectinolytic microorganisms as important contributors to flax retting and shows that environmental conditions affect both microbial succession and the degradation pathway [7,8,16]. However, the available studies do not provide a validated moisture-management strategy for oilseed flax straw under the hot and dry conditions characteristic of the study region. In particular, quantitative relationships between short-term moistening, subsequent moisture loss during field spreading, microbial abundance, and final fiber quality have not been established for the cultivars investigated here.

The knowledge gap addressed in this study is therefore not the general feasibility of biological flax retting, which is already established, but the lack of an experimentally supported process model for maintaining a moisture regime sufficient for microbial retting of oilseed flax straw under field conditions. A second gap concerns the integration of moisture kinetics with quantitative microbiological and fiber quality data to identify when continued retting becomes technologically undesirable.

The present study addresses these gaps by combining (i) measurements of stem water uptake and desorption, (ii) cultivar-specific mathematical modeling of moisture kinetics, (iii) quantitative culture-based assessment of cellulolytic and pathogenic microbiota together with species occurrence, and (iv) direct evaluation of retted-straw separation and fiber mechanical properties. The study includes three oilseed flax cultivars—Pivdenna Nich, Aisberg, and Debut—and the fiber flax cultivar Charivnyi.

2. Materials and Methods

The field experiments followed the principle of a single difference: soil preparation, sowing, crop care, and harvesting were performed on the same day using identical implements. Five independent field replicates were established, with a replicate plot area of 1 ha. The plant material comprised three oilseed flax cultivars (Pivdenna Nich, Aisberg, and Debut) and the fiber flax cultivar Charivnyi, which was included as a reference material.

The field experiments were conducted during July–August in 2022–2025. Field spreading was observed for 8 consecutive days. During the double-moistening treatment, the spread stems were artificially moistened twice per day using a 10 min moistening operation at each application; the original experiment did not report fixed clock times for these applications. Meteorological observations from the Kherson weather station showed mean daytime air temperatures of 31.5–35.0 °C and mean nighttime temperatures of 23.3–25.6 °C; mean daytime relative humidity was 21.0–28.5%, and mean nighttime relative humidity

was 54.0–64.5% across the four study years (Table 1). These values describe environmental exposure rather than a controlled incubation regime. Air temperature and relative humidity during field spreading were not actively controlled.

Table 1. Meteorological parameters during the study years (based on data from the Kherson weather station).

Meteorological Parameters (July–August)	Year, Mean Values			
	2022	**2023**	**2024**	**2025**
Air temperature, °C				
Daytime	31.5	34.0	35.0	32.0
Nighttime	23.3	23.4	25.6	23.6
Relative air humidity, %				
Daytime	28.5	21.0	22.5	27.5
Nighttime	64.5	58.0	54.0	59.5

2.1. Plant Material and Experimental Design

Because continuous hourly temperature and relative humidity records and exact clock times of each moistening event were not reported in the original experimental dataset, these variables cannot be treated as controlled constants. The reported models therefore describe empirical relationships within the documented July–August environmental range and should not be interpreted as temperature-independent or universally transferable process equations.

2.2. Stem Water Uptake and Desorption Experiments

Moisture absorption was measured after artificial moistening for 10–90 min at 10 min intervals. At each interval, five 10 g stem samples were collected from different parts of the experimental spread according to the sampling approach [17]. Samples were weighed before moistening and after each exposure interval; the dry mass was determined after drying to constant mass. Moisture desorption was monitored for 24 h after moistening, with measurements at 1 h. intervals during the first 12 h and at 24 h.

Moisture content on a dry-mass basis was calculated as:

$$W = \frac{m_w – m_d}{m_d} \times 100, \quad (1)$$

where W is moisture content on a dry-mass basis (%), m_w is the mass of the wet sample (kg), and m_d is the mass of the oven-dry sample (kg). Thus, W = 100% means that the mass of water equals the oven-dry mass; values above 100% indicate that the water mass exceeds the dry matter mass. This quantity should not be confused with relative humidity (RH), which is the ratio of actual to saturation water-vapor pressure in air and is reported separately as a percentage.

The water-uptake rate was calculated as the first derivative of the measured moisture-content curve with respect to time:

$$v_w = \frac{dW}{d\tau}, \quad (2)$$

where v_w is the water-uptake rate (% min^{-1}), W is moisture content on a dry-mass basis (%), and τ is time (min). Because v_w is the derivative of W(τ), no independent empirical rate data were generated; the rate curves were calculated from the fitted moisture-

content functions. This definition distinguishes water uptake by the stem from atmospheric relative humidity.

Experimental data were processed in PTC Mathcad Prime 11 and CurveExpert Professional 2.7.1. Candidate functions were fitted by least squares. Approximately 20 candidate functions were evaluated for each experimental series. Functions with discontinuities or physically implausible behavior within the experimental interval were excluded. The remaining models were compared using R^2, RMSE, MAE, and inspection of residuals and fitted-versus-observed trajectories. R was retained only as a descriptive measure of linear association and was not used alone to establish adequacy of a nonlinear model [11,12,18–20].

2.3. Microbiological Analysis

Culturable microorganisms were isolated by the moist-chamber method. Pieces of flax straw (0.5–1.0 cm) were placed on sterile filter paper in Petri dishes containing 2–3 sterile paper disks moistened with sterile water. Plates were maintained at 26 °C and examined microscopically for colony and mycelial development. Pure fungal cultures were isolated where possible and identified by morphological characteristics. Parallel isolation was performed on wort agar and potato–glucose agar [7–10,21].

Quantitative enumeration of culturable microbiota was performed by serial dilution and plate counting. One gram of finely cut flax straw was suspended in 90 mL sterile water and mixed for 5–10 min. Ten-fold serial dilutions were prepared, and 1 mL of the appropriate dilution was plated in duplicate or triplicate. Approximately 20 mL of molten agar cooled to 40 °C was added to each plate. Plates were incubated for 7–12 days under the conditions specified for the respective medium and examined from day 3 onward.

Colony abundance was calculated as:

$$N = \frac{a \times b}{x}, \quad (3)$$

where N is the culturable abundance (units g^{-1}), a is the number of colonies counted, b is the dilution factor, and x is the number of replicate plates/tubes. The reported values represent culturable abundance rather than total microbial abundance.

Quantification of cellulolytic microorganisms was also performed by serial dilution. One gram of finely cut straw was suspended in 90 mL sterile water and mixed for 5–10 min. Aliquots were inoculated into Hutchinson medium containing a cellulose (filter-paper) strip. Three replicate tubes were prepared for each dilution. Tubes were incubated for 10 days at 37 °C, and cellulose decomposition was evaluated using the McCrady approach [7–10,21].

Hutchinson medium composition (g L^{-1} unless otherwise stated): K_2HPO_4, 1.0; $CaCl_2$, 0.1; $MgSO_4 \cdot 7H_2O$, 0.3; NaCl, 0.1; $FeCl_3$, 0.01; $NaNO_3$, 2.5; pH 7.2–7.3.

After inoculation, the tubes were incubated for 10 days at 37 °C. Cellulose decomposition was recorded, and viable-cell abundance was estimated using the McCrady tables [7–10,21]. Because the study used culture-based methods, the reported values represent culturable abundance rather than total microbial abundance. Detection in a culture assay does not by itself demonstrate that a taxon was actively degrading cellulose or pectin under the field conditions.

2.4. Retted-Straw and Fiber Quality Assessment

To assess the effect of spreading duration and moistening regime on retted straw and fiber quality, samples were conditioned to a standard moisture content of 19% by drying to constant mass. Retting degree was quantified as fiber-to-wood separation using an OOV device; a separation value $\geq$4.1 units was classified as normal retting. Fiber strength was determined using a DKV-60 dynamometer. Flexibility was measured with a GV-2 flexometer using 30 fiber bundles (60 measurements), and the arithmetic mean was

calculated. Fiber content was determined gravimetrically after mechanical separation of the fiber fraction from the woody core using an ML-5 laboratory breaker.

For each treatment, separation, strength, and flexibility were measured in five replicates. The results are reported as arithmetic means, and absolute and relative deviations were calculated to describe experimental variability.

The technologically relevant spreading duration was identified by jointly considering retting degree (fiber-to-wood separation) and fiber quality (strength and flexibility). The selected duration was the shortest period at which normal retting was achieved while acceptable mechanical properties were retained.

2.5. Mathematical Modeling, Model Equations, and Evaluation Criteria

Trend models were used to describe moisture-content trajectories as functions of time. Candidate functions were fitted to the experimental time series by least squares. The supplied model-output file contains rational, power, exponential, and polynomial-rational expressions evaluated over t = 0–25 or t = 0–90 time units, depending on the experimental series. Because the supplied output file does not identify every expression by cultivar and response variable, the equations are reported only where their correspondence to the original worksheet can be established; unsupported cultivar-specific assignments have been removed.

The supplied model-output file contains rational, power, exponential, and polynomial-rational expressions evaluated over t = 0–25 or t = 0–90 time units, depending on the experimental series. Because the supplied output file does not identify every expression by cultivar and response variable, the fitted expressions are retained in the corresponding model tables without assigning unsupported equation numbers or cultivar-specific labels. The attached reviewer calculation shows that direct evaluation of some supplied expressions can produce values above 100 at t = 1; therefore, these expressions must be checked against the original raw data and plotting worksheet before they are interpreted as final predictive equations. The present manuscript treats them as empirical candidate functions rather than validated universal models.

The model-selection criteria were R^2, RMSE, MAE, and residual behavior. r was reported descriptively but was not treated as a sufficient adequacy criterion for nonlinear regression. Model selection was performed separately for each experimental series. A common functional form across cultivars is therefore interpreted only as a shared empirical shape within the tested dataset, not as evidence of a universal cultivar-independent model [19,20].

The modeling workflow comprised: (i) inspection of the experimental time series; (ii) generation of approximately 20 candidate functions; (iii) least-squares parameter estimation; (iv) exclusion of functions with discontinuities or implausible behavior within the experimental interval; (v) calculation of R^2, RMSE, and MAE; (vi) inspection of residuals and fitted-versus-observed trajectories; (vii) selection of the best-supported function for each experimental series; and (viii) comparison of predicted and measured values. Environmental variables were not entered as independent predictors. The raw point-by-point residuals were not retained in the supplied model-output file; therefore, the manuscript does not claim a formal residual normality or independence test.

The water-uptake experiments showed that the measured water content on a dry-mass basis approached approximately 100% within 10 min of moistening, after which the increase became substantially slower. This inflection-like change was used operationally to identify the end of the rapid initial uptake phase. It is not sufficient, by itself, to conclude that free-water adsorption had ended or that bound-water absorption had begun. Without direct

measurements of surface water, capillary filling, or water-binding states, the mechanistic interpretation remains provisional.

After moistening, moisture content on a dry-mass basis declined rapidly during field exposure, reaching approximately 64–73% after 1 h and 25–34% after 12 h, with values approaching the initial level after 24 h. These observations provide an empirical basis for repeated moistening under the documented July–August field conditions. Recent work likewise shows that water uptake and drying behavior of flax stems depend on retting stage and moisture exposure, supporting the use of explicit water-content kinetics rather than relative humidity terminology for the stem measurements [22].

The combined moisture, microbiological, and material-quality results indicate that twice-daily artificial moistening supported continued development of culturable microorganisms during field spreading. The quantitative data demonstrate temporal changes in cultured cellulolytic and taxa classified as plant-pathogenic in the literature, while species-occurrence data indicate changes in community structure. Because enzyme activity, total microbial DNA, and cell-wall composition were not directly measured, these findings support process association rather than a fully resolved causal mechanism.

Under the tested conditions, 5 days of spreading represented the experimentally supported processing duration: fiber-to-wood separation reached 6.8 units, mean fiber strength was 17.8 daN, and flexibility was approximately 34.0 mm. The result applies to the investigated cultivars, the twice-daily 10 min moistening regime, the 8-day observation period, and the documented environmental conditions. It should not be generalized as a universal retting duration or universal mathematical model for other cultivars, locations, seasons, or moisture regimes.

The selected empirical functions were used to describe the observed kinetics of stem water uptake and desorption and to support the timing of repeated moistening during field spreading. Transferability is limited to the tested cultivars, the experimental moisture regime, and the documented July–August environmental range. Universality beyond these conditions was not assumed.

2.6. Evaluation Metrics and Notation

The principal evaluation metrics were defined as follows: $R^2 = 1 - \Sigma(y_i - \hat{y}_i)^2/\Sigma(y_i - \bar{y})^2$; RMSE = [$\Sigma(y_i - \hat{y}_i)^2/n$]^{1/2}; and MAE = $\Sigma\,|y_i - \hat{y}_i|/n$. Here, y_i is the measured response, $\hat{y}_i$ is the model-predicted response, $\bar{y}$ is the mean measured response, and n is the number of observations. R^2 is dimensionless; RMSE and MAE have the same units as the response variable. The correlation coefficient r is reported only as a descriptive measure of linear association and is not used as the sole criterion for nonlinear model adequacy [19,20].

The standard definitions used for model checking were:

$$R^2 = 1 - \Sigma(y_i - \hat{y}_i)^2/\Sigma(y_i - \bar{y})^2; \quad (4)$$

$$\text{RMSE} = [\Sigma(y_i - \hat{y}_i)^2/n]^{\wedge}\{1/2\}; \quad (5)$$

$$\text{MAE} = \Sigma\,|y_i - \hat{y}_i|/n. \quad (6)$$

These definitions are consistent with standard forecasting practice [19,20].

Here, y_i is the measured value, $\hat{y}_i$ is the model-estimated value, $\bar{y}$ is the arithmetic mean of the measured values, and n is the number of observations; r is dimensionless, while RMSE and MAE have the same units as the response variable.

3. Results

Relative stem moisture was measured at defined moistening intervals. Mean values for the three oilseed flax cultivars Pivdenna Nich, Aisberg, and Debut and the fiber flax cultivar Charivnyi are presented in Table 2 and Figure 1.

Table 2. Dependence of flax-stem moisture content on moistening duration (dry-mass basis).

Moistening Time, min	Relative Moisture Content of Flax Stems, %			
	Oilseed Flax Cultivar Pivdenna Nich	Oilseed Flax Cultivar Aisberg	Oilseed Flax Cultivar Debut	Fiber Flax Cultivar Charivnyi
0	8.1	6.7	8.4	9.4
10	101.1	98.7	98.5	99.6
20	108.4	105.3	104.2	106.4
30	110.1	108.6	107.4	105.2
40	112.4	110.3	110.1	115.6
50	114.6	112.1	113.6	121.1
60	119.4	117.5	118.6	126.4
70	127.0	123.6	125.4	129.3
80	133.2	131.0	134.5	137.4
90	139.0	135.7	141.1	144.1

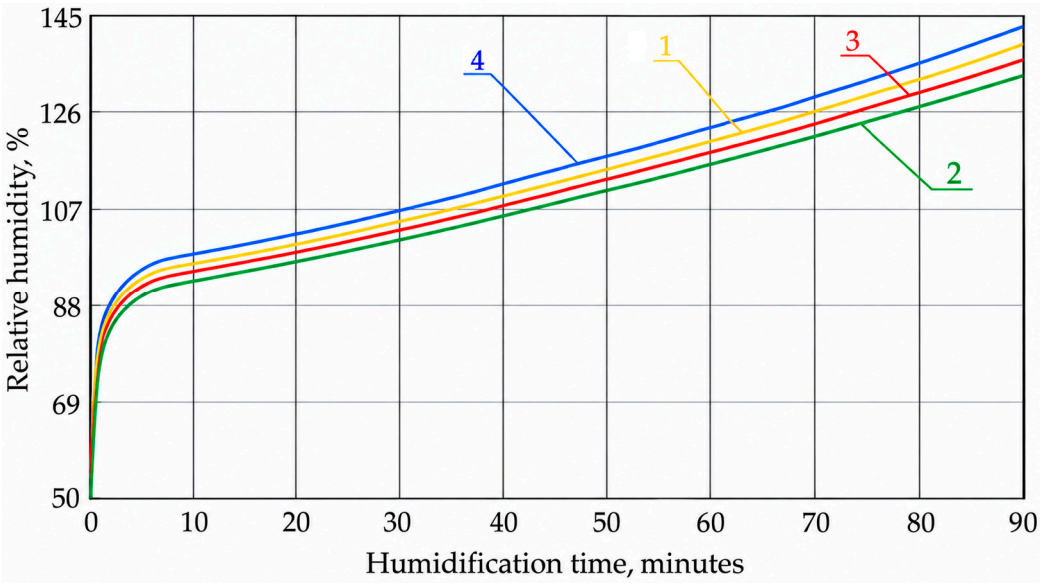


Figure 1. Dependence of flax-stem moisture content on moistening duration for oilseed flax varieties Pivdenna Nich (1), Aisberg (2), Debut (3), and fiber flax variety Charivnyi (4).

The experimentally measured mean moisture-content values are reported in Table 2. The fitted curves in Figures 1–3 are empirical descriptions of the observations and should be distinguished from the measured data; they do not replace the experimental measurements. For clarity, the figures should display the original measured values as markers and the fitted relationships as separate lines, using the existing experimental dataset.

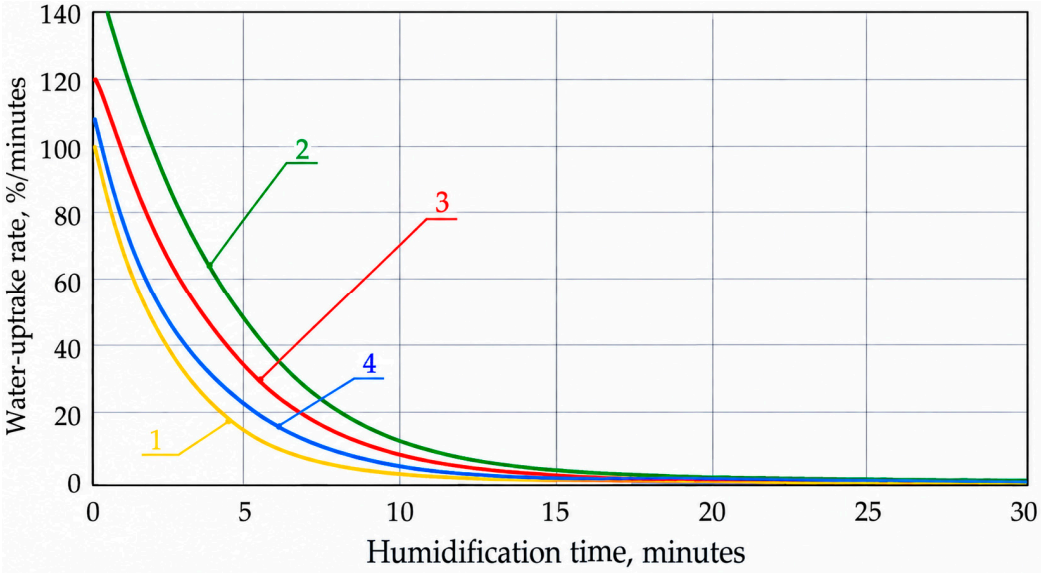


Figure 2. Dependence of stem water-uptake rate on moistening duration for oilseed flax varieties Pivdenna Nich (1), Aisberg (4), Debut (3), and fiber flax variety Charivnyi (2).

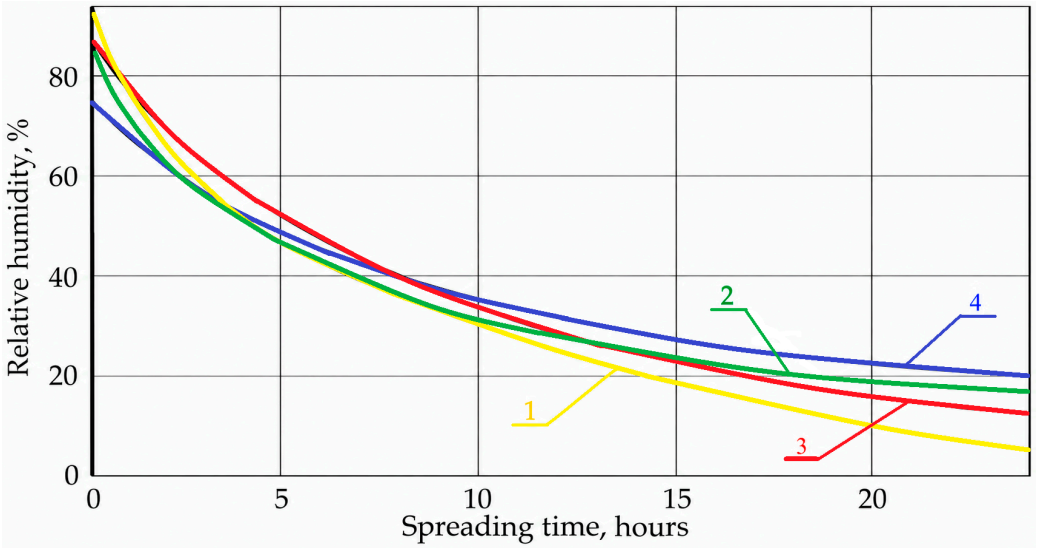


Figure 3. Dependence of flax-stem moisture content on spreading duration during desorption for oilseed flax varieties Pivdenna Nich (1), Aisberg (2), Debut (3), and fiber flax variety Charivnyi (4).

As a result of the mathematical processing of the experimental data, candidate models were obtained for the oilseed flax varieties Pivdenna Nich, Aisberg, and Debut, as well as for the fiber flax variety Charivnyi. Models with discontinuities in the technological interval were excluded. Among the remaining models, selection was based on R^2, RMSE, MAE, and residual behavior; r was used only descriptively. The detailed fitted functions and their parameters are presented in Tables 3 and 4.

To utilize the obtained dependencies as trend models for forecasting the dynamics of the technological process, the best-supported empirical model was selected for each experimental series. For the tested flax varieties, the rational functional form reported in Table 4 provided the best-supported description within the available model set; this does not imply that the same parameters or functional form will necessarily apply to other varieties or environments.

$$y(x) = \frac{a + b \cdot x}{1 + c \cdot x + d \cdot x^2}. \quad (7)$$

Table 3. Mathematical models of moisture absorption for flax straw stems. Mathematical models of moisture absorption for flax straw stems oilseed flax cultivar Pivdenna Nich.

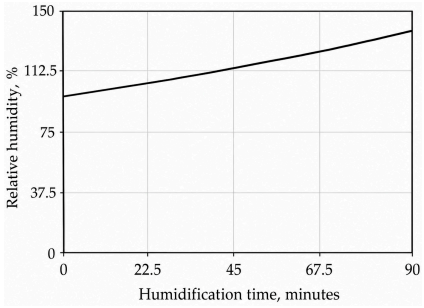
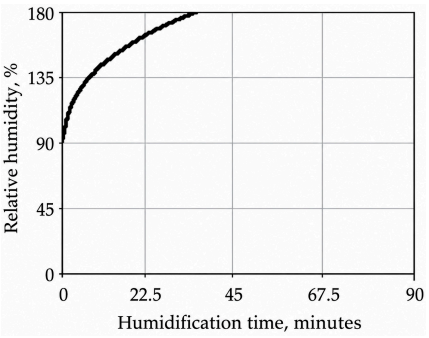
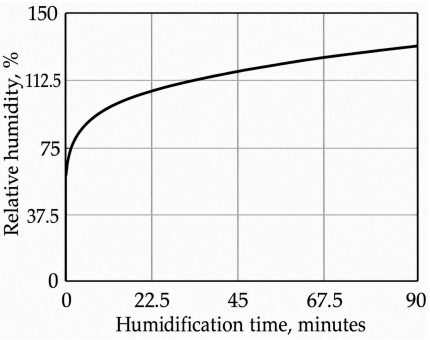
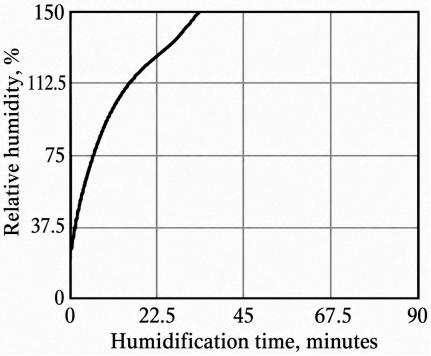
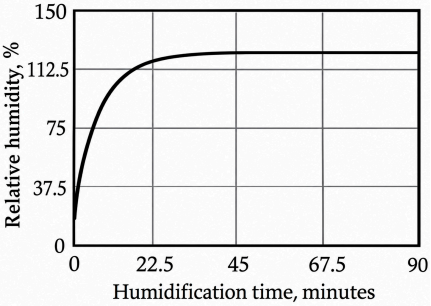
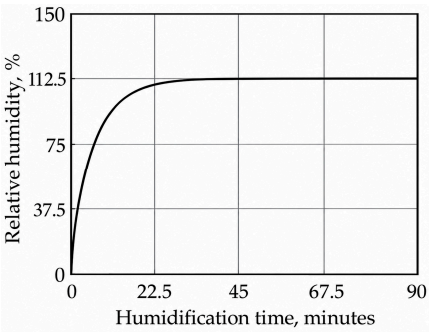
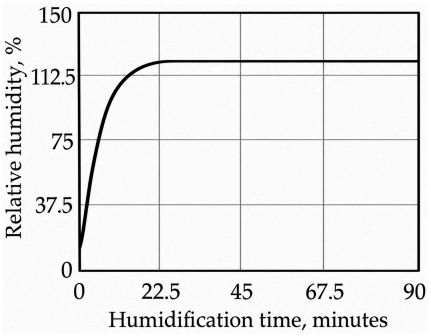
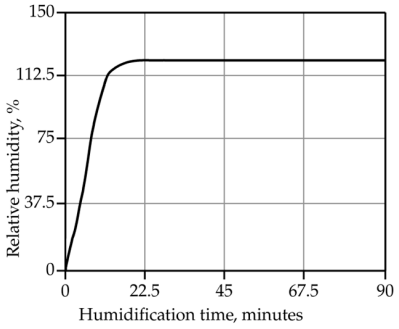
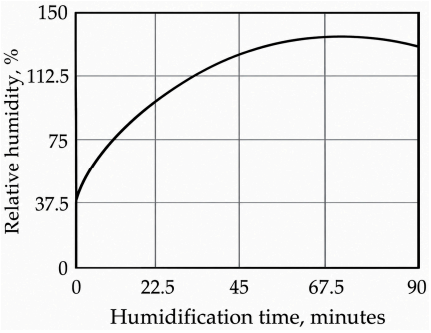
#	Function	Correlation Coefficient, r, and Root-Mean-Square Deviation, S	Graph
1	Rational Function $y_1^{PN}(t) = \frac{8.10+74{,}231{,}239\cdot t}{1+752{,}940.61\cdot t-2392.77\cdot t^2}$	r = 0.999 S = 2.096	
2	Harris Model $y_2^{PN}(t) = \frac{1}{0.12-0.11\cdot t^{0.012}}$	r = 0.994 S = 4.691	
3	MMF Model $y_3^{PN}(t) = \frac{8.25\cdot 10.74+721.20\cdot t^{0.18}}{10.74+t^{0.18}}$	r = 0.991 S = 5.708	
4	Polynomial Fit $y_4^{PN}(t) = 12.97 + 10.77\cdot t - 0.38\cdot t^2 + 0.005\cdot t^3 - 2.53\cdot t^4$	r = 0.984 S = 8.686	
5	Exponential Association $y_5^{PN}(t) = 122.00\cdot(1.08 - e^{-0.15\cdot t})$	r = 0.964 S = 10.362	

Table 3. *Cont.*

#	Function	Correlation Coefficient, r, and Root-Mean-Square Deviation, S	Graph
6	Exponential Association $y_6^{PN}(t) = 113.29 \cdot (1.07 - e^{-0.14t})$	r = 0.967 S = 10.562	
7	Gompertz Relation $y_7^{PN}(t) = 121.02 \cdot e^{-e^{0.95-0.25t}}$	r = 0.964 S = 11.099	
8	Logistic Model $y_8^{PN}(t) = \frac{120.61}{1+12.93 \cdot e^{-0.42t}}$	r = 0.963 S = 11.299	
9	Quadratic Fit $y_9^{PN}(t) = \frac{121.01}{(1+e^{-3.06-0.26t})^{\frac{1}{0.02}}}$	r = 0.964 S = 11.995	

The four cultivars showed a broadly similar overall increase in stem moisture during the first 10 min of moistening, followed by a slower uptake phase (Figure 1). However, the fitted parameters differed among cultivars. Therefore, the similarity of the curves is interpreted as a shared empirical trajectory within the tested material set rather than evidence that the process is independent of cultivar.

For a more precise description of the rapid initial uptake phase, the water-uptake rate was calculated as the time derivative of the fitted moisture-content functions. This derivative-based approach avoids treating the rate as an independently measured response.

Table 4. Fitted empirical models for stem moisture content during water uptake for the studied flax varieties.

Flax Variety	Mathematical Relationship	Correlation Coefficient, r	Root-Mean-Square Deviation, S
Pivdenna Nich	$y_{BII1}^{PN}(t) = \frac{8.10+74{,}231{,}239 \cdot t}{1+752{,}940.61 \cdot t-2392.77 \cdot t^2}$	0.999	2.096
Aisberg	$y_{BII1}^{A}(t) = \frac{6.7+6{,}068{,}895{,}800 \cdot t}{1+62{,}891{,}074 \cdot t-200{,}040.27 \cdot t^2}$	0.999	1.951
Debut	$y_{BII1}^{D}(t) = \frac{8.48+1.4722529 \cdot 10^{10} \cdot t}{1+1.5534089 \cdot 10^{8} \cdot t-557{,}934.51 \cdot t^2}$	0.999	1.805
Charivnyi	$y_{BII1}^{C}(t) = \frac{9.4+280.33 \cdot t}{1+2.82 \cdot t-0.0099 \cdot t^2}$	0.999	2.254

The mean values are presented in Table 5.

Table 5. Dependence of flax-stem moisture-absorption rate on moistening duration.

Moistening Time, min	Relative Moisture Content of Flax Stems, %			
	Oilseed Flax Cultivar Pivdenna Nich	Oilseed Flax Cultivar Aisberg	Oilseed Flax Cultivar Debut	Fiber Flax Cultivar Charivnyi
10	9.30	9.20	9.01	9.02
20	0.73	0.66	0.527	0.68
30	0.17	0.33	0.33	0.12
40	0.23	0.17	0.27	1.04
50	0.22	0.18	0.35	0.55
60	0.48	0.54	0.50	0.53
70	0.76	0.61	0.68	0.29
80	0.62	0.74	0.91	0.81
90	0.58	0.47	0.69	0.67

Approximately twenty candidate models were evaluated for each studied variety. Functions with discontinuities within the technological interval were excluded. The remaining models were compared using R^2, RMSE, MAE, and residual behavior. The Exponential Fit and Modified Power forms provided the best-supported descriptions for the corresponding experimental series and are reported in Table 5.

$$y(x) = a \cdot e^{b \cdot x}, \quad (8)$$

$$y(x) = a \cdot b^{x}. \quad (9)$$

The water-uptake-rate relationships are shown in Figure 2 and correspond to the derivatives of the fitted moisture-content functions reported in Tables 3 and 4.

For oilseed flax variety Pivdenna Nich:

$$V_{ma}^{PN}(t) = 113.68 \cdot e^{-0.25 \cdot t}. \quad (10)$$

Correlation coefficient r = 0.985, root-mean-square deviation S = 0.493.

For oilseed flax variety Aisberg:

$$V_{ma}^{A}(t) = 118.69 \cdot e^{-0.26 \cdot t}. \quad (11)$$

Correlation coefficient r = 0.986, root-mean-square deviation S = 0.469.
For oilseed flax variety Debut:

$$V_{ma}^{D}(t) = 130.81 \cdot 0.77^{\cdot t}. \quad (12)$$

Correlation coefficient r = 0.979, root-mean-square deviation S = 0.553.
For fiber flax variety Charivnyi:

$$V_{ma}^{C}(t) = 113.91 \cdot 0.78^{\cdot t}. \quad (13)$$

Correlation coefficient r = 0.976, root-mean-square deviation S = 0.594.

Analysis of the water-uptake-rate curves indicates that the rate increased sharply at the beginning of moistening and then decreased. From approximately 10 to 90 min, the measured water-content increase was substantially slower. The change in slope is therefore interpreted as a transition from rapid initial wetting and penetration into stem tissues to a slower water-uptake regime. The present measurements do not distinguish quantitatively between surface adsorption, capillary uptake, and absorption into plant tissues; consequently, the terms "adsorption" and "absorption" are not used as mechanistic conclusions unless directly supported by the measurement method.

Considering the documented July–August field conditions, the reverse process—desorption of retained water from the straw stems—was investigated to determine how long moisture was retained and whether one moistening operation at the beginning of retting could maintain a sufficient moisture level throughout the day.

The results of the 24 h flax-stem water desorption experiment are summarized in Tables 6 and 7.

As a result of the mathematical processing of the experimental data, mathematical models of the moisture desorption process were obtained. Excluding the models with insufficient correlation coefficient values, we obtain for oilseed flax varieties Pivdenna Nich—six models, Aisberg—nine models, Debut—12 models, and for fiber flax variety Charivnyi—three models. These models have a high degree of correlation and a minimum root-mean-square deviation, which are sufficient for performing engineering calculations.

Table 6. Change in flax-stem moisture content during desorption (dry-mass basis).

Moisture Release Time, Hours	Relative Moisture Content of Flax Stems, %			
	Oilseed Flax Cultivar Pivdenna Nich	Oilseed Flax Cultivar Aisberg	Oilseed Flax Cultivar Debut	Fiber Flax Cultivar Charivnyi
0	101.1	98.7	98.6	99.6
1	72.6	69.1	72.1	64.7
2	61.5	60.9	64.7	61.4
3	57.1	56.1	61.3	57.7
4	54.2	54.9	57.2	55.1
5	49.7	51.2	54.4	53.8
6	46.4	48.7	51.0	50.1
7	42.5	45.1	48.8	47.7
8	38.7	41.1	45.6	44.5
9	35.2	37.5	40.9	40.2
10	33.9	34.0	38.2	38.1
11	28.6	31.8	35.9	36.5
12	25.1	27.4	33.4	32.0
24	8.1	6.7	8.4	9.4

Table 7. Mathematical models of moisture desorption for flax straw stems. Mathematical models of moisture desorption for flax straw stems oilseed flax cultivar Pivdenna Nich.

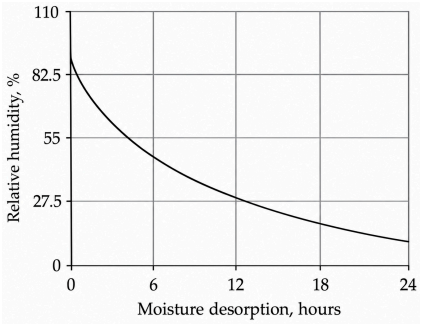
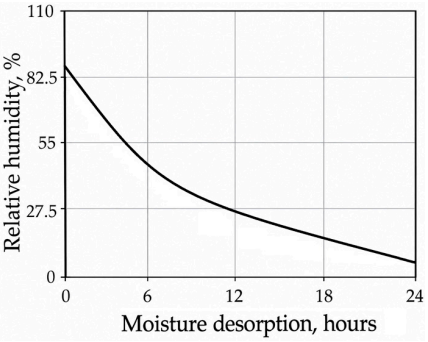
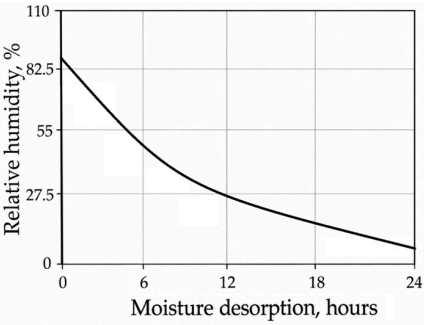
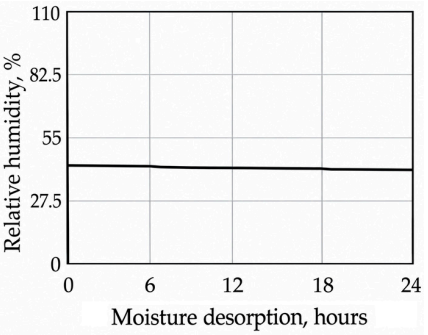
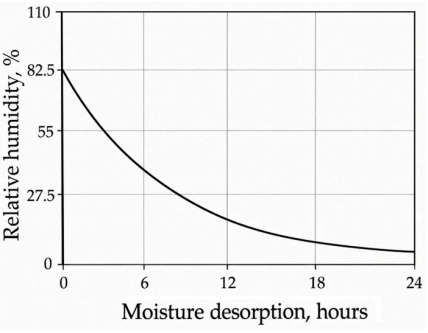
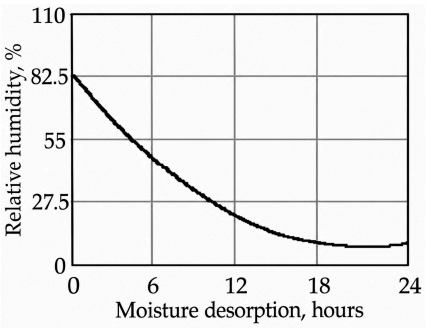
#	Function	Correlation Coefficient, r, and Root-Mean-Square Deviation, S	Graph
1	MMF Model $y_{BB1}^{PN}(t) = \frac{101.02 \cdot 56.36 - 1540.31t^{0.39}}{56.36 + t^{0.39}}$	r = 0.99 S = 2.88	
2	Modified Power $y_{BB}^{PN}(t) = 86.84 \cdot 0.89^{t}$	r = 0.97 S = 5.84	
3	Exponential Fit $y_{BB}^{PN}(t) = 86.84 \cdot e^{(-0.11t)}$	r = 0.97 S = 5.84	
4	Richards Model $Y_{BB1}^{PN} = \frac{171.02}{1 + e^{(17.86 + 2.8 \cdot t)^{\left(\frac{1}{26.35}\right)}}}$	r = 0.97 S = 5.93	
5	Quadratic Fit $y_{BB}^{PN}(t) = 83.56 - 7.03t + 016t^{2}$	r = 0.96 S = 6.62	

Table 7. *Cont.*

#	Function	Correlation Coefficient, r, and Root-Mean-Square Deviation, S	Graph
6	Sinusoidal Fit $y_{BB}^{PN}(t) = 349.89 + 341.58 \cdot \cos(0.03t + 2.47)$	r = 0.95 S = 6.75	

To generalize the results of the desorption experiment, candidate models were compared using R^2, RMSE, MAE, and residual behavior. The models with the best-supported statistics and physically plausible trajectories over the experimental interval are presented in Table 8. A graphical representation of these fitted relationships is shown in Figure 3.

Table 8. Mathematical models of the moisture desorption process for the stems of the studied flax varieties.

Flax Variety	Mathematical Relationship	Correlation Coefficient, r	Root-Mean-Square Deviation, S
Pivdenna Nich	MMF Model: $y_{BB1}^{PN}(t) = \frac{101.02 \cdot 56.36 - 1540.31 \cdot t^{0.39}}{56.36 + t^{0.39}}$	0.998	1.697
Aisberg	Harris Model: $y_{BB1}^{A}(t) = \frac{1}{0.01 + 0.0027 \cdot t^{0.86}}$	0.972	5.526
Debut	Logistic Model: $y_{BB1}^{D}(t) = \frac{-45.08}{1 - 1.51 \cdot e^{0.04 \cdot t}}$	0.974	5.164
Charivnyi	Rational Function: $y_{BB1}^{C}(t) = \frac{99.6 - 1.05 \cdot 10^{11} \cdot t}{1 - 1.39 \cdot 10^{9} \cdot t - 1.40 \cdot 10^{8} \cdot t^2}$	0.978	4.764

Analysis of the data in Table 8 and Figure 3 indicates that, 12 h after moistening, the moisture content of the spread flax stems of the studied varieties averages 30%. Over time, the moisture content of the spread flax stems gradually decreases and, after 24 h, equals their initial moisture content. Therefore, as the research results show, additional moistening should be carried out no later than 12 h after the first moistening.

Based on these observations, under the July–August field conditions represented by the Kherson weather-station means (daytime 31.5–35.0 °C and 21.0–28.5% RH; nighttime 23.3–25.6 °C and 54.0–64.5% RH), a single moistening at the beginning of the technological process was insufficient to maintain the measured stem moisture content over 24 h.

The desorption-rate curves therefore provide an empirical basis for determining the interval between moistening operations under the documented field conditions. Because temperature and atmospheric RH were not experimentally controlled and continuous hourly meteorological records were not available in the study dataset, the observed interval should not be interpreted as a universal physical constant or generalized beyond the tested environmental range.

To examine the association between artificial moistening and microbial development, the species composition and quantitative abundance of culturable microorganisms developing on flax stems were investigated [8,23–26].

For microbiological comparison, oilseed flax stems from the spread layer without artificial moistening were used as the control. Samples were collected from representative locations within the experimental spread layer at the designated sampling times. The species composition was assessed by culture and morphological identification, whereas quantitative abundance was determined by serial-dilution counts. The field experiment comprised five independent plot replicates; 2–3 Petri dishes were used for each dilution in the plate-count procedure and three tubes per dilution were used for the cellulolytic assay.

Tables 9 and 10 present the results of the study of the species and quantitative composition of microbiota developing on flax stems in the control variant and with single moistening of the spread layer of the ribbon.

Table 9. Change in the species composition of microbiota during the spreading process in the control variant and with single moistening.

Species Composition	Spreading Duration, Hours			
	Control Variant		Single Moistening	
	12	24	12	24
Alternaria linicola	-	r/f	r/f	f/f
Ascochuta linicola	-	-	r/f	-
Bipolaris gorokiniana	-	-	-	-
Cladosporium herbarum	-	r/f	r/f	f/f
Colletotrichum lini	-	r/f	r/f	f/f
Dothiorela gregaria	-	-	-	f/f
Fusarium gibosum	-	-	-	r/f
Fusarium graminear	-	-	-	r/f
Gonatobotrys flava	-	-	r/f	r/f
Septoria linicola	-	-	r/f	f/f

Note: r/f—rarely found, occurrence rate less than 30%; f/f—frequently found, occurrence rate 30–50%.

Table 10. Quantitative composition of microbiota: control variant and with single moistening.

Type of Microflora	Spreading Duration, Hours			
	Control Variant		Single Moistening	
	12	24	12	24
Cellulolytic, thousand units/g	-	45	60	150
Pathogenic, units/g	-	-	120	300

The species composition and quantitative abundance differed between the control and the single-moistening treatment. In the moistened treatment, culturable fungi associated in the literature with pectin degradation, including *Alternaria linicola*, *Cladosporium herbarum* and *Colletotrichum lini*, were detected more frequently, whereas their occurrence in the unmoistened control was limited (Tables 9 and 10).

The first day of spreading under single moistening was characterized by the appearance and increase in the cultured fungal groups listed in Table 9. These observations indicate that moistening changed the culturable microbial community relative to the control. The designation of taxa as pectin-associated reflects documented associations in the literature and does not constitute a direct measurement of pectinolytic enzyme activity under the present field conditions.

The data in Tables 9 and 10 indicate that, under the climatic conditions studied, the absence of artificial moistening was associated with limited development of the culturable microbiota. The increased occurrence and abundance of pectin-associated fungal taxa after moistening are consistent with a more favorable moisture regime for microbial development, but culture-based measurements do not establish the magnitude of their metabolic contribution to retting.

Therefore, in this study, an investigation was carried out on the microbiota developing on the stems of the spread ribbon with the application of a double artificial moistening operation in order to determine how favorable and effective the application of a repeated moistening operation is for the development of pectinolytic microbiota.

At the beginning of spreading, the straw of all variants was under equal conditions; therefore, data on the species composition of microorganisms for each variety are not presented separately, since for all studied oilseed flax varieties, the process of converting straw into retted flax occurs similarly. Repeated moistening, as shown by the results of the study of the moisture desorption process, was carried out at 12 h intervals, with each moistening lasting 10 min, when the stem moisture content was at least 30%. Significant changes in the species and quantitative composition of microbiota began to occur after the first day of spreading.

Table 11 presents the species-occurrence data for each day of spreading under the double-moistening treatment.

Table 11. Change in the species composition of microbiota during the spreading process with double moistening.

Species Composition	Spreading Duration, Days							
	1	**2**	**3**	**4**	**5**	**6**	**7**	**8**
Alternaria linicola	f/f	f/f	f/f	dom.	dom.	dom.	dom.	dom.
Cladosporium herbarum	f/f	f/f	dom.	dom.	dom.	f/f	f/f	f/f
Colletotrichum lini	dom.	dom.	dom.	dom.	dom.	dom.	dom.	f/f
Fusarium gibosum	–	–	r/f	r/f	r/f	r/f	f/f	f/f
Fusarium raminear	–	–	r/f	–	–	–	–	–
Fusarium venaceum	–	–	–	–	–	r/f	–	–
Gonatobotris flava	–	–	r/f	r/f	r/f	f/f	f/f	f/f
Septoria linicola	r/f	–	r/f	r/f	r/f	f/f	f/f	f/f

Note: r/f—rarely found, occurrence rate less than 30%; f/f—frequently found, occurrence rate 30–50%; dom.—dominant, occurring with a frequency of more than 50%.

With double moistening, *Alternaria linicola*, *Cladosporium herbarum* and *Colletotrichum lini* were detected frequently during days 1–3 and were dominant by days 4–5. In contrast, *Fusarium avenaceum* and *Fusarium graminear* were not detected during the observed period, while *Gonatobotrys flava* and *Septoria linicola* were detected less frequently during the early stages. *Fusarium gibosum* was first detected on day 3 and occurred at a frequency below 30% through day 5. These observations describe taxon occurrence; the functional labels pectinolytic or cellulolytic are based on published characteristics of the respective taxa rather than direct enzyme-activity measurements in this study.

From days 6–8, the pectin-associated taxa *Alternaria linicola*, *Cladosporium herbarum* and *Colletotrichum lini* remained frequent or dominant, while the abundance of taxa classified in the study as cellulolytic or pathogenic increased. *Gonatobotrys flava* and *Septoria linicola* occurred at frequencies of 30–50%, and *Fusarium gibosum* reached 30–50% during days 7–8. The term “pathogenic” is used here to denote taxa recognized in the literature as associated with plant disease; their presence in the samples does not by itself demonstrate pathogenic activity or causation of fiber deterioration under the tested retting conditions.

The quantitative data likewise show a marked increase in the cultured cellulolytic and pathogenic groups during days 6–8 (Table 12). These counts support a change in the composition and abundance of culturable microorganisms during the later stages of spreading, rather than a direct measurement of the enzymatic activity of individual taxa.

Table 12. Quantitative composition of microbiota during the spreading process with double moistening.

Type of Microflora	Spreading Duration, Days							
	1	**2**	**3**	**4**	**5**	**6**	**7**	**8**
Cellulolytic, thousand units/g	180	195	210	219	280	564	790	930
Pathogenic, units/g	365	384	405	420	506	758	960	1240

4. Discussion

4.1. Moisture Modeling and Process Transferability

The moisture-uptake results show that all four tested cultivars reached approximately 98.5–101.1% water content on a dry-mass basis after 10 min of moistening, followed by a much slower increase during the subsequent 80 min. The common rational functional form selected for the tested series should be interpreted as an empirical description of the observed dataset rather than a mechanistic or universal model. The fitted parameters and residual deviations differ among cultivars. The present study did not measure cellulose, hemicellulose, pectin, lignin, or other cell-wall fractions, so cultivar differences cannot be attributed mechanistically to cellulose content or other internal components.

The desorption data provide the operational basis for repeated moistening. After the initial moistening, water content declined from approximately 99–101% to about 64–73% within 1 h and continued to decrease to approximately 25–34% by 12 h, returning close to the initial level after 24 h. Because field temperature and atmospheric RH were not experimentally controlled and continuous hourly records were not reported, this result should be interpreted as an observed field-specific water-retention pattern rather than a universal physical constant.

The modeling approach is therefore best viewed as an empirical process-control tool. Its strength is the quantitative description of observed water-content trajectories; its limitation is that temperature, RH, solar radiation, precipitation, and straw composition were not included as independent predictors. A multifactor model and independent validation dataset would be required to test whether the fitted relationships remain stable across seasons, locations, and genotypes.

4.2. Microbial Dynamics and Technological Implications

The culture-based data show a temporal shift in the culturable microbial community under double moistening. *Alternaria linicola*, *Cladosporium herbarum*, and *Colletotrichum lini* were frequently detected during days 1–3 and were dominant at several observations during days 4–5. In parallel, the quantitative cellulolytic group increased from 180 thousand units g−1 on day 1 to 930 thousand units g−1 on day 8, while the group classified as pathogenic increased from 365 to 1240 units g−1 over the same period. These data demonstrate changes in culturable abundance and occurrence, but they do not establish direct enzyme activity by the detected taxa.

4.3. Limitations and Evidence for the Retting Optimum

The microbiological interpretation remains deliberately conservative. The labels “pectin-associated”, “cellulolytic”, and “pathogenic” refer to documented functional or ecological associations of the detected taxa [7,8,21,23]; the present study did not directly

measure pectinolytic or cellulolytic enzyme activity, total microbial DNA, or degradation of individual cell-wall polymers. Therefore, the data demonstrate changes in culturable abundance and occurrence, not direct causal rates of pectin or cellulose degradation. Experimental evidence linking cultivar-specific model parameters to cell-wall composition would require additional compositional and enzymatic measurements.

The 5-day processing duration is supported by direct material measurements: the mean fiber-to-wood separation increased to 6.8 units by day 5, while the mean fiber strength remained at 17.8 daN and flexibility increased to approximately 34.0 mm. The observed rise in cellulolytic and pathogenic abundance after day 5 provides microbiological context for limiting further spreading, but it is not by itself proof of cellulose degradation. The processing duration therefore applies specifically to the tested cultivars, the twice-daily 10 min moistening regime, the 8-day observation window, and the environmental conditions documented for the Kherson weather station in July–August 2022–2025.

5. Conclusions

Water uptake by the tested flax stems reached approximately 98.5–101.1% on a dry-mass basis within 10 min of moistening. Subsequent water gain was substantially slower, indicating that the first 10 min captured the dominant initial uptake phase under the tested conditions. The observed change in slope is treated as an operational transition in uptake kinetics rather than proof of a change from free-water adsorption to bound-water absorption.

Water loss reduced stem moisture by approximately 27–36 percentage points during the first hour and to approximately 25–34% by 12 h, with moisture approaching the initial level after 24 h. These observations support a twice-daily moistening schedule for the tested field conditions; they do not establish a universal schedule for other climates.

The rational function provided the best-supported empirical functional form within the tested moisture-uptake datasets, but the fitted parameters differed among cultivars. Accordingly, the study supports a common empirical functional form within the tested material set rather than a universal cultivar-independent model. Testing of additional genotypes, climates, raw-data residuals, and independent validation datasets is required before broader generalization.

Under twice-daily artificial moistening for 10 min at approximately 12 h intervals, pectin-associated taxa were frequent or dominant during the first 5 days, whereas cellulolytic and plant-pathogenic culturable groups increased after day 5. Direct measurements of retting degree and fiber properties support 5 days as the experimentally supported processing duration for the tested cultivars and environmental conditions. The study did not directly measure cell-wall composition or enzyme activity; therefore, proposed mechanisms involving cellulose preservation or degradation should be considered hypotheses for future mechanistic validation.

Author Contributions: Conceptualization, O.G. and S.L.; methodology, O.G.; validation, O.G., S.L. and N.L.; formal analysis, O.G. and S.L.; investigation, O.G.; data curation, O.G.; writing—original draft preparation, O.G. and S.L.; writing—review and editing, O.G., S.L. and N.L.; supervision, O.G. and S.L.; project administration, S.L. All authors have read and agreed to the published version of the manuscript.

Funding: The authors declare that this research received no external funding.

Institutional Review Board Statement: Not applicable.

Informed Consent Statement: Informed consent was obtained from all subjects involved in the study.

Data Availability Statement: Data are available from the corresponding author upon reasonable request. Requests for the dataset should be addressed via email.

Conflicts of Interest: The authors declare no conflicts of interest.

References

1. Horach, O.O.; Lavrenko, N.M. Development of scientific foundations for obtaining bast fiber fillers for the production of technical textiles. In *Scientific Monograph: Modern Agronomy Trends: Innovation, Sustainable Development and the Future of Agriculture*; Baltija Publishing: Riga, Latvia, 2025; pp. 58–81. [CrossRef]
2. Lavrenko, S.; Gorach, O.; Lavrenko, N. Research on the Adhesive Properties of Flax Fiber in the Production of Composite Materials. *Technologies* **2025**, *13*, 582. [CrossRef]
3. Harsányi, J.; Poraj-Kobielska, M.; Wedwitschka, H.; Tirsch, M.; Kretzschmar, J. Controlled anaerobic water retting of flax as part of an innovative biorefinery process. *Biomass Convers. Biorefinery* **2025**, *15*, 16499–16510. [CrossRef]
4. Mukherjee, S.; Goulas, E.; Creach, A.; Krzewinski, F.; Galinousky, D.; Blervacq, A.-S.; D'Arras, P.; Ratahiry, S.; Menuge, A.; Soulat, D.; et al. Metaproteomics identifies key cell wall degrading enzymes and proteins potentially related to inter-field variability in fiber quality during flax dew retting. *Ind. Crops Prod.* **2024**, *222*, 119907. [CrossRef]
5. Mukherjee, S.; Goulas, E.; De Waele, I.; Créach, A.; Hawkins, S.; Grec, S.; Blervacq, A.-S. Tracking flax dew retting by infrared vibrational spectroscopy combined with a powerful multivariate statistical analysis. *Ind. Crops Prod.* **2025**, *236*, 120798. [CrossRef]
6. Mukherjee, S.; Galinousky, D.; Blervacq, A.-S.; Buchaillot, L.; Arscott, S.; Grec, S. Spectral colour changes: A promising parameter for smart flax dew retting monitoring solutions. *Comput. Electron. Agric.* **2026**, *221*, 111407. [CrossRef]
7. Horach, O. Scientific foundations of complex processing and use of stalks and seeds of oil flax. In *Modern Plant Production Technologies in the Face of Climate Change*; Publishing House of the Adam Chętnik Scientific Society in Ostrołęka: Ostrołęka, Poland, 2025; pp. 58–156.
8. Zhang, C.; Cai, B.; Sun, Y.; Kang, J.; Pei, F.; Ge, J. Microbial communities that drive the degradation of flax pectin and hemicellulose during dew retting with Bacillus licheniformis HDYM-04 and Bacillus subtilis ZC-01 addition. *Bioresour. Technol.* **2023**, *371*, 128516. [CrossRef] [PubMed]
9. Reda, A.; Dargent, T.; Thomas, L.; Grec, S.; Buchaillot, L.; Arscott, S. The influence of dew retting on the mechanical properties of single flax fibers measured using micromechanical and nanomechanical approaches. *Fibers* **2024**, *12*, 91. [CrossRef]
10. Różańska, W.; Romanowska, B.; Rojewski, S. The quantity and quality of flax and hemp fibers obtained using the osmotic, water-, and dew-retting processes. *Materials* **2023**, *16*, 7436. [CrossRef] [PubMed]
11. Chabbert, B.; Padovani, J.; Djemiel, C.; Ossemond, J.; Lemaître, A.; Yoshinaga, A.; Hawkins, S.; Grec, S.; Beaugrand, J.; Kurek, B. Multimodal assessment of flax dew retting and its functional impact on fibers and natural fiber composites. *Ind. Crops Prod.* **2020**, *148*, 112255. [CrossRef]
12. Angulu, M.; Gusovius, H.-J. Retting of bast fiber crops like hemp and flax—A review for classification of procedures. *Fibers* **2024**, *12*, 28. [CrossRef]
13. Chursina, L.A.; Tikhosova, G.A.; Horach, O.O.; Yanyuk, T.I. *Scientific Foundations of Complex Processing of Stalks and Seeds of Oil Flax*; Kherson: Oldi-plu, Ukraine, 2011; 356p.
14. Gorach, O.; Dombrovska, O.; Tikhosova, A. Development of resource-saving technologies for obtaining composite materials based on the use of oilseed flax fibers. *Inmateh-Agric. Eng.* **2021**, *65*, 275–282. [CrossRef]
15. Gorach, O.; Dombrovska, O.; Tikhosova, A. Scientific development of innovative technologies of obtaining composite materials from of oilseed flax fibers. *Vlákna A Text.* **2021**, *28*, 25–30.
16. Gorach, O.; Dzyundzya, O.; Rezvykh, N. Innovative Technology for the production of gluten-free food products of a new generation. *Curr. Nutr. Food Sci.* **2024**, *20*, 734–744. [CrossRef]
17. Ushkarenko, V.O.; Naidenova, V.O.; Laser, P.N.; Svyrydov, O.V.; Lavrenko, S.O.; Lavrenko, N.M. *Scientific Research in Agronomy: A Textbook*; Hrin, D.S.: Kherson, Ukraine, 2016; 316p.
18. Hyndman, R.J.; Athanasopoulos, G. *Forecasting: Principles and Practice*, 3rd ed.; OTexts: Melbourne, Australia, 2021. [CrossRef]
19. Petropoulos, F.; Makridakis, S.; Stylianou, N.; Assimakopoulos, V. Forecasting: Theory and practice. *Int. J. Forecast.* **2022**, *38*, 705–871. [CrossRef]
20. Ragoubi, M.; Lecoublet, M.; Khennache, M.; Atanase, L.I.; Poilâne, C.; Leblanc, N. How retting could affect the mechanical behavior of flax/epoxy biocomposite materials? *Materials* **2023**, *16*, 2929. [CrossRef] [PubMed]
21. Hasan, R.; Aktar, N.; Kabir, S.M.T.; Honi, U.; Halim, A.; Islam, R.; Sarker, M.D.H.; Haque, M.S.; Alam, M.M.; Islam, M.S. Pectinolytic bacterial consortia reduce jute retting period and improve fibre quality. *Sci. Rep.* **2020**, *10*, 5174. [CrossRef] [PubMed]
22. Reda, A.; Buchaillot, L.; Arscott, S. Drying Behavior of Flax Stems at Different Degrees of Dew Retting Under Simulated Rainfall: Implications for Smart Agriculture and Sensor Development. *Agriculture* **2025**, *15*, 395. [CrossRef]

23. Das, B.; Chakraborty, D.; Saha, A.; Ray, D.P. Quality optimization of flax fibre through durational management of water retting technology under sub-tropical climate. *Ind. Crops Prod.* **2021**, *162*, 113277. [CrossRef]
24. Zimniewska, M.; Różańska, W.; Kicińska-Jakubowska, A.; Mańkowski, J.; Wiśniewski, M.; Dziedziczak, K.; Baraniecki, P. Influence of the hydrodynamic degumming process on the quality of decorticated flax fibers. *Text. Res. J.* **2022**, *92*, 3360–3371. [CrossRef]
25. Wang, X.; Li, Y.; Zhang, H.; Zhao, D.; Ge, J. Response characteristics of flax retting liquid addition during chicken manure composting: Focusing on core bacteria in organic carbon mineralization and humification. *Bioresour. Technol.* **2023**, *381*, 129112. [CrossRef] [PubMed]
26. Tu, X.; Kang, J.; Zhang, C.; Qiu, W.; Guo, Y.; Ao, G.; Ge, J.; Ping, W. Effect of combined bacteria on the flax dew degumming process: Substance degradation sequence and changes in functional bacteria taxa. *Int. J. Biol. Macromol.* **2024**, *273*, 132877. [CrossRef] [PubMed]

Disclaimer/Publisher's Note: The statements, opinions and data contained in all publications are solely those of the individual author(s) and contributor(s) and not of MDPI and/or the editor(s). MDPI and/or the editor(s) disclaim responsibility for any injury to people or property resulting from any ideas, methods, instructions or products referred to in the content.